

ADDENDUM 2 TO P253

A high sensitivity investigation of K_S and neutral hyperon decays using a modified K_S beam.

R. Batley, A. Bevan, R.S. Dosanjh, T.J. Gershon, G.E. Kalmus¹, D.J. Munday, E. Olaiya, M.A. Parker, S.A. Wotton

Cavendish Laboratory, University of Cambridge, Cambridge, CB3 0HE, U.K.²

G. Barr, G. Bocquet, J. Bremer, A. Ceccucci, T. Cuhadar, D. Cundy, N. Doble, V. Falaleev, L. Gatignon, A. Gonidec, B. Gorini, G. Govi, P. Grafström, W. Kubischta, A. Lacourt, M. Lenti³, A. Norton, B. Panzer-Steindel, D. Schinzel, G. Tatishvili⁴, H. Taureg, H. Wahl

CERN, CH-1211 Geneva 23, Switzerland.

C. Cheshkov, A. Gaponenko, P. Hristov, V. Kekelidze, D. Madigojine, N. Molokanova, Yu. Potrebenikov, A. Tkatchev, A. Zinchenko

Joint Institute for Nuclear Research, Dubna, Russian Federation.

C. Lazzeroni⁵, V. Martin, R. Sacco, A. Walker

Department of Physics and Astronomy, University of Edinburgh, JCMB King's Buildings, Mayfield Road, Edinburgh, EH9 3JZ, U.K.

W. Baldini, D. Bettoni, R. Calabrese, M. Contalbrigo, P. Dalpiaz, J. Duclos, E. Luppi, P.L. Frabetti, A. Gianoli, M. Martini, F. Petrucci, M. Savrié

Dipartimento di Fisica dell'Università e Sezione dell'INFN di Ferrara, I-44100 Ferrara, Italy.

A. Bizzeti⁶, F. Beccatini, M. Calvetti, G. Collazuol, G. Graziani, E. Iacopini, F. Martelli⁷, M. Veltri⁷

Dipartimento di Fisica dell'Università e Sezione dell'INFN di Firenze, I-50125 Firenze, Italy.

M. Eppard, K. Holtz, K. Kleinknecht, U. Koch, L. Köpke, P.Lopes da Silva, P. Marouelli, I. Pellmann, A. Peters, B. Renk, S.A. Schmidt, Y. Shué, K. Talleur, R. Wanke, A. Winhart, M. Wittgen

Institut für Physik, Universität Mainz, D-55099 Mainz, Germany⁸.

G. Anzivino, P. Cenci, P. Imbergamo, P. Lubrano, A. Mestvirishvili, A. Nappi, M. Pepe, M. Piccini, M. Valdata

Dipartimento di Fisica dell'Università e Sezione dell'INFN di Perugia, I-06100 Perugia, Italy.

L. Bertanza, A. Bigi, R. Carosi, R. Casali, C. Cerri, M. Cirilli, F. Costantini, R. Fantechi, S. Giudici, I. Mannelli, G. Pierazzini, M. Sozzi

¹Based at Rutherford Appleton Laboratory

²Funded by the U.K. Particle Physics and Astronomy Research Council.

³On leave from Sezione dell'INFN di Firenze, I-50125 Firenze, Italy.

⁴On leave from Joint Institute for Nuclear Research, Dubna, 141980, Russian Federation

⁵From Jan 1, 2000 with Cambridge

⁶Dipartimento di Fisica dell'Università di Modena e Reggio Emilia, via G. Campi 213/A I-41100 Modena, Italy

⁷Istituto di Fisica - Università di Urbino - via S. Chiara, 27 - I-61029 Urbino (PS) Italy

⁸Funded by the German Federal Minister for Research and Technology (BMBF) under contract 7MZ18P(4)-TP2.

J.B. Cheze, M. De Beer, P. Debu, G. Marel, E. Mazzucato, B. Peyaud, R. Turlay, B. Vallage
DSM/DAPNIA - CEA Saclay, F-91191 Gif-sur-Yvette, France.

M. Holder, A. Maier, M. Ziolkowski
Fachbereich Physik, Universität Siegen, D-57068 Siegen, Germany⁹.

R. Arcidiacono, C. Biino, N. Cartiglia, R. Guida, F. Marchetto, E. Menichetti, N. Pastrone
*Dipartimento di Fisica Sperimentale dell'Università e Sezione dell'INFN di Torino,
I-10125 Torino, Italy.*

W. Wislicki
*Soltan Institute for Nuclear Studies, Laboratory for High Energy Physics,
PL-00-681 Warsaw, Poland¹⁰.*

H. Dibon, M. Jeitler, M. Markytan, I. Mikulec, G. Neuhofer, M. Pernicka, A. Taurok
*Österreichische Akademie der Wissenschaften, Institut für Hochenergiephysik,
A-1050 Wien, Austria.*

1 Introduction

We propose to use the NA48 detectors and a slightly modified beam line to search for very rare K_S decays. The sensitivity of the experiment will also allow us to perform systematic studies on several less rare K_S decays and on the neutral hyperon decays at sensitivities greatly in excess of current values. Lists of some of the rare K_S and hyperon decays accessible to this experiment are given in Table 1 and in Table 3 respectively. Table 1 also includes the contamination from K_L decays in the K_S beam. During a short test performed in 1999, a proton intensity on the K_S target 200 times that used in standard $\Re(\epsilon'/\epsilon)$ running was achieved, and data were collected. By minor optimisation of the beam and operating at a proton energy of 400 GeV, 400 times the standard proton flux should be achievable without changing the NA48 detector. The single event sensitivity (SES) for one year's exposure¹¹ for K_S channels is estimated to be $\frac{1}{\alpha}(3 \times 10^{-11})$, where α is the total acceptance of the channel after all necessary cuts. In the case of $K_S \rightarrow \pi^0 e^+ e^-$, α has been calculated to be 0.05, thus giving an SES of 6×10^{-10} for this channel. This value is a factor of about 500 lower than the present published limit.

A modest upgrade to some of the front end electronics/read-out systems is currently being studied, and might result in a factor two improvement in the achievable SES.

The following sections 2-5 describe the principal decay modes and parameters addressed by the proposed experiment.

2 $K_S \rightarrow \pi^0 e^+ e^-$

The interest of $K_S \rightarrow \pi^0 e^+ e^-$ is that it enables one to place a bound on the indirect CP violating term in the $K_L \rightarrow \pi^0 e^+ e^-$ decay.

⁹Funded by the German Federal Minister for Research and Technology (BMBF) under contract 056SI74.

¹⁰Supported by the Committee for Scientific Research grant 2P03B07615 and using computing resources of the Interdisciplinary Center for Mathematical and Computational Modelling of the University of Warsaw.

¹¹120 days at 50% efficiency

There are three contributions to the $K_L \rightarrow \pi^0 e^+ e^-$ decay: direct CP violating, indirect CP violating, and CP conserving. The CP conserving contribution can be obtained by measuring the low $m_{\gamma\gamma}$ component for the $K_L \rightarrow \pi^0 \gamma\gamma$ decay. The direct and the indirect contribution interfere, and their relative contribution to the branching ratio can be written as [1]:

$$\text{BR}(K_L \rightarrow \pi^0 e^+ e^-) \times 10^{12} = 15.3 a_s^2 - 6.8 a_s \frac{\Im m(\lambda_t)}{10^{-4}} + 2.8 \left(\frac{\Im m(\lambda_t)}{10^{-4}} \right)^2, \quad (1)$$

where $\Im m(\lambda_t) = V_{ts}^* V_{td}$ is the relevant combination of CKM matrix elements which describe the short distance CP violation. The a_s parameter describes the strength of the indirect CP violating component in the $K_L \rightarrow \pi^0 e^+ e^-$ decay. It is related to $\text{BR}(K_S \rightarrow \pi^0 e^+ e^-)$ via the relation:

$$\text{BR}(K_S \rightarrow \pi^0 e^+ e^-) = 5.2 \times 10^{-9} |a_s|^2 \quad (2)$$

According to naive dimensional analysis in chiral perturbation theory, $a_s \sim O(1)$. However, the prediction does not have any degree of confidence, so it is clearly important to measure $\text{BR}(K_S \rightarrow \pi^0 e^+ e^-)$ experimentally.

The present proposal, with no upgrades to the detector read-out, would yield about 7 events at $a_s = 1$. The physics interest for the $K_S \rightarrow \pi^0 \mu^+ \mu^-$ is the same as for the electron channel. However, the backgrounds to this channel are quite different. The decay rate is suppressed by about a factor of 5 due to phase space.

2.1 Backgrounds to $K_S \rightarrow \pi^0 e^+ e^-$

Backgrounds have been considered from both K_S and K_L channels. It should be noted that there are about 4×10^7 K_L decays per K_S lifetime per year.

1. Background from $K_L \rightarrow e^+ e^- \gamma\gamma$

The experimental branching ratio is:

$$\text{BR}(K_L \rightarrow e^+ e^- \gamma\gamma (E_\gamma^* > 5 \text{ MeV})) \simeq 6 \times 10^{-7} \quad (3)$$

The number of these events accepted per year (15% acceptance) in three K_S lifetimes is:

$$6 \times 10^{-7} \times 0.15 \times 12 \times 10^7 \simeq 11 \quad (4)$$

A cut on $m_{\gamma\gamma}$ of ± 2.5 MeV around the π^0 mass reduces this number by a factor of 30, *i.e.*, we would expect $\leq \frac{1}{3}$ of an event from this background source if no other kinematic cuts are made. Very loose cuts can easily reduce this by a factor of 2 or more without affecting the $K_S \rightarrow \pi^0 e^+ e^-$ acceptance significantly.

2. Background from $K_S \rightarrow e^+ e^- \gamma\gamma$

Although the branching ratio of $K_S \rightarrow e^+ e^- \gamma\gamma$ has not been measured, an estimate can be made starting from the measured value of $\text{BR}(K_S \rightarrow \gamma\gamma)$. This estimate gives:

$$\text{BR}(K_S \rightarrow e^+ e^- \gamma\gamma (E_\gamma^* > 5 \text{ MeV})) \sim 1.3 \times 10^{-9} \quad (5)$$

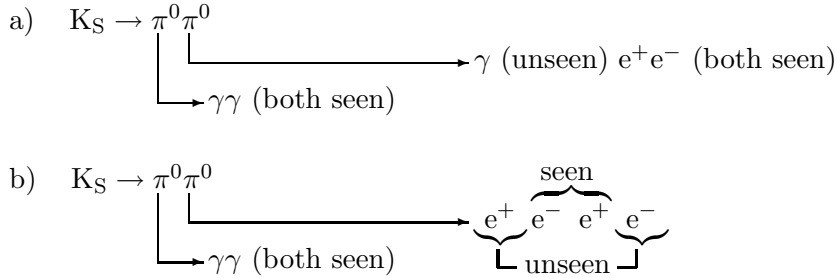
There are a total of 3×10^{10} K_S mesons decaying per year in the fiducial volume. With an estimated acceptance of this background channel of 15%, the total number of background events accepted per year is:

$$1.3 \times 10^{-9} \times 0.15 \times 3 \times 10^{10} \sim 6 \quad (6)$$

If the same $m_{\gamma\gamma}$ cut is made around the π^0 mass as for $K_L \rightarrow \pi^0 e^+ e^-$, then this number is reduced by a factor of 30, *i.e.*, we would expect $\leq 1/5$ of a background event from this source. As in the case $K_L \rightarrow \pi^0 e^+ e^-$, very modest kinematic cuts can reduce this to less than 1/10 of a background event.

3. Backgrounds from $K_S \rightarrow \pi^0 \pi^0_{Dalitz}$ (or double Dalitz)

The potential background from single and double Dalitz decay of one of the pions from the above prolific decay mode is being studied using Monte Carlo simulation.



Although a larger Monte Carlo sample is needed to fine tune the necessary cuts to eliminate this background, present indications are that it can be reduced to negligible proportions.

3 $K_S \rightarrow \gamma\gamma$ and $K_S \rightarrow \pi^0 \gamma\gamma$

The study of the decays $K_{S,L} \rightarrow \gamma\gamma$ and $K_{S,L} \rightarrow \pi^0 \gamma\gamma$ is important for understanding the low energy hadron dynamics of Chiral Perturbation Theory (χ PT), since they are sensitive to higher order loop effects [2]. At present only the K_L modes of these decays have been measured precisely. NA31 has measured a branching ratio of $K_S \rightarrow \gamma\gamma$ to be $(2.4 \pm 0.9) \times 10^{-6}$, and $K_S \rightarrow \pi^0 \gamma\gamma$ has not yet been observed. The decay $K_S \rightarrow \gamma\gamma$ is especially interesting because χ PT predicts unambiguously that the branching ratio is (2.25×10^{-6}) , with an error of less than 10%. Hence a precision measurement of this mode is an important test of χ PT.

In the proposed high intensity K_S beam, a precision measurement of $K_S \rightarrow \gamma\gamma$ can be performed. The first 7 m length after the K_S collimator is free from background coming from $K_S \rightarrow \pi^0 \pi^0$ decays. The $K_L \rightarrow \gamma\gamma$ contamination in the signal can be estimated precisely by measuring the K_L flux coming from $K_L \rightarrow \pi^0 \pi^0 \pi^0$ decays in the beam. We have calculated that $\simeq 24,000$ $K_S \rightarrow \gamma\gamma$ events will be observed for 3×10^{10} K_S decays in the decay region.

The branching ratio of $K_S \rightarrow \pi^0 \gamma\gamma$ is estimated to be about 4×10^{-8} . Using a 15 m fiducial region after the K_S collimator, it is calculated that 114 $K_S \rightarrow \pi^0 \gamma\gamma$ will be observed for 3×10^{10} K_S decays. The detected signal is expected to have a contamination of about 30% from $K_L \rightarrow \pi^0 \gamma\gamma$ decays. This contribution can again be estimated precisely by measuring the K_L flux with $K_L \rightarrow \pi^0 \pi^0 \pi^0$ decays.

4 Sensitivity to the parameter η_{000}

The $\pi^0\pi^0\pi^0$ final state has a well-defined CP eigenvalue, and therefore the decay $K_S \rightarrow \pi^0\pi^0\pi^0$ does not occur if CP is conserved. The CP-violation parameter η_{000} is defined as the ratio of K_S to K_L decay amplitudes:

$$\eta_{000} = \frac{A(K_S \rightarrow \pi^0\pi^0\pi^0)}{A(K_L \rightarrow \pi^0\pi^0\pi^0)} \quad (7)$$

Under CPT invariance, $\Re(\eta_{000})$ is given by the CP violation in the $K^0\bar{K}^0$ mixing and the imaginary part is sensitive to direct CP violation in a decay amplitude. In addition, η_{000} provides an important experimental input to a test of CPT symmetry based on the Bell-Steinberger relation which couples the CPT violating parameter Δ to the sum of the products of K_S and K_L decay amplitudes [3]:

$$(1 + i \tan \phi_{SW})[\Re(\epsilon) - i\Im(\Delta)] = \sum_f \alpha_f. \quad (8)$$

In the above ϕ_{SW} is the superweak phase with $\tan \phi_{SW} = 2\Delta m/(\Gamma_S - \Gamma_L)$ and $\alpha_f = A^*(K_S \rightarrow f)A(K_L \rightarrow f)/\Gamma_S$. The α_f are directly proportional to the corresponding CP violating parameter η_f (with the exception of α_{l3}). Their current world averages are listed in Table 2. One of the main uncertainties in the α_f sum is the error on α_{000} , i.e. η_{000} . Therefore not only evidence for CP violation in $K_S \rightarrow \pi^0\pi^0\pi^0$, but already a better limit on η_{000} would improve the test of CPT symmetry. Currently, the best measurement of η_{000} is the one reported by the CPLEAR Collaboration: $\Re(\eta_{000}) = (0.18 \pm 0.15)$ and $\Im(\eta_{000}) = (0.15 \pm 0.20)$, corresponding to a limit on the branching ratio of $\mathcal{B}(K_S \rightarrow \pi^0\pi^0\pi^0) < 1.9 \times 10^{-5}$ at 90% CL [4]. More recently the SND collaboration has lowered the limit on the branching fraction to 1.4×10^{-5} at 95% CL [5].

We plan to improve the above limits on the real and imaginary part of η_{000} by a factor of ten from the measurement of K_S - K_L interference near the production target. The $3\pi^0$ intensity as a function of proper time is given by:

$$I_{3\pi^0} = K \times \Gamma(K_L \rightarrow 3\pi^0) \times \left(e^{-t/\tau_L} + |\eta_{000}|^2 e^{-t/\tau_S} + 2D|\eta_{000}| e^{-t/2(1/\tau_S+1/\tau_L)} \cos(\Delta mt + \phi_{000}) \right), \quad (9)$$

where D is the $K^0\bar{K}^0$ dilution at production (about 0.3 for NA48) and K is the acceptance. The sensitivity to η_{000} comes from the interference term which is superimposed on a very large, flat $K_L \rightarrow \pi^0\pi^0\pi^0$ component. The maximum interference is at the target, and most of the effect is contained within two K_S lifetimes as it can be seen in Figure 1. The disadvantage of losing the first lifetime due to the presence of the collimator is offset in part by the very good proper time resolution ($\sim 0.1 c\tau_S$) provided by the combination of high energy beams and high resolution calorimetry. To evaluate the sensitivity to η_{000} , we have used samples of $3\pi^0$ from a K_S -only high intensity run, and from Monte Carlo simulation. Our sensitivity will allow to put bounds on η_{000} to $\sim 1\%$ with one year of data taking. To keep the systematic error under control, our technique relies on a good knowledge of the acceptance. The sensitivity of $\Re\eta_{000}$ and $\Im\eta_{000}$ on the knowledge of the acceptance is shown in Figure 2. We plan to use large $K_L \rightarrow 3\pi^0$ samples collected during the $\Re(\epsilon'/\epsilon)$ measurement to cross-check the Monte Carlo calculation of the acceptance, and we feel that the systematic error on the knowledge of the acceptance can be kept at the level of $\sim 10^{-3}/c\tau_S$.

5 Hyperon decays

A detailed list of hyperon decays which are accessible is shown in Table 3. The most significant measurements are briefly described below.

1. Hyperon electro-magnetic mass splitting

The hyperon electro-magnetic mass splittings amongst the SU(3) octet members are now accessible to lattice calculations [6]. The NA48 detector with its high-resolution photon detector enables a very precise measurement the mass of the Ξ^0 . From a first analysis of the 1997 data and using the mean value for the mass of the Ξ^- [7], we obtain:

$$M(\Xi^-) - M(\Xi^0) = (6.50 \pm 0.25) \text{ MeV},$$

at variance with the lattice result 5.68 ± 0.24 MeV. With a high intensity run in the K_S neutral beam and additional systematic studies on the energy calibration, we will be able to reduce the experimental uncertainty to 0.1 MeV, which is the current error on $M(\Xi^-)$.

2. Hyperon radiative decays

Radiative hyperon decays between flavour octet states are allowed by isospin conservation in SU(3)-symmetric models. The Σ^0 and Λ are orthogonal three quark states with different isospin. In this way, the study of the radiative decays $\Xi^0 \rightarrow \Lambda\gamma$ and $\Xi^0 \rightarrow \Sigma\gamma$ gives information about SU(3)-breaking effects. Since non-leptonic weak interactions are complicated by hadronic effects, different model calculations result in branching ratios ranging over an order of magnitude. Our first results from the 1997 run, based on 31 and 20 events, respectively, are:

$$\begin{aligned} \text{BR}(\Xi^0 \rightarrow \Lambda\gamma) &= (1.90 \pm 0.34(\text{stat}) \pm 0.19(\text{syst})) \times 10^{-3} \\ \text{BR}(\Xi^0 \rightarrow \Sigma\gamma) &= (3.14 \pm 0.76(\text{stat}) \pm 0.32(\text{syst})) \times 10^{-3} \end{aligned}$$

These agree with one model based on SU(6) symmetry and vector dominance [8]. In this proposed high intensity run, we intend to increase the event sample by a factor of 100, reduce the systematic error by a factor of 2, and obtain a result with 5% uncertainty.

3. Hyperon β decays

The β decay of the Ξ^0 hyperon ($\Xi^0 \rightarrow \Sigma^+ e^- \bar{\nu}$), with a branching ratio of 2.5×10^{-4} , can be detected in NA48 by identifying the electron in the LKr calorimeter and the Σ^+ by its decay to $p\pi^0$ (51%). We expect to collect 25000 events in the proposed run. These events will be used for a new consistency check of SU(3) symmetry and the Cabibbo model in hyperon decays (F/D couplings).

4. Search for $\Xi^0 \rightarrow p\pi^-$

This decay with a double strangeness change ($\Delta S = 2$) should exist in the second order weak interactions. The present experimental limit is a branching ratio $\leq 4 \times 10^{-5}$ at 90% CL, and this can be improved by a factor of 100.

6 The intense K_S beam

6.1 Introduction

The present layout of beams to experiment NA48, shown in Figure 3, comprises simultaneous, nearly-collinear K_L and K_S beams designed for the $\Re(\epsilon'/\epsilon)$ measurement [9]. The K_S beam is

derived from a small fraction ($\sim 3 \times 10^7$ out of 1.5×10^{12}) of the primary protons per SPS pulse used to produce the K_L . These protons are selected via channeling in a bent silicon crystal [10]. Within the same layout, it is possible to move the K_L production target out of the beam and to direct the protons, without loss, past the crystal and directly onto the K_S target. In the absence of interactions on the upstream target and beam dump and without decays from the K_L beam passing through the detector, it is possible to increase the intensity of the K_S beam by a large factor (~ 200 -500) compared to that of the K_S component of the simultaneous beams.

6.2 Proton transport to K_S target

The primary proton beam issuing from target station T4 is attenuated and collimated to a flux less than 10^{11} protons per SPS pulse by the dump/collimators (TAX) at the beginning of the P42 beam line leading to the North Area High Intensity Area (TCC8+ECN3), where the kaon beams and the NA48 detectors are installed. Further collimators in the upstream section of this beam line are used to redefine the beam and to select the flux of protons to produce the K_S . This proton beam then travels without further loss along the existing K12 beam line, and is finally focused and directed onto the K_S production target at an angle (at present 4.2 mrad) with respect to the subsequent beam axis, as shown in Figure 4.

6.3 The K_S beam

The layout of the K_S beam is shown schematically in Figure 4. The target is located in vacuum, 72 mm vertically above the axis of the present K_L beam. It consists of a 2 mm diameter, 400 mm long rod of beryllium. The target and the following collimator apertures are precisely aligned along an axis pointing downwards at 0.6 mrad, which intersects the horizontal (K_L) axis and passes through the centre of the detectors at a longitudinal distance of 120 m from the target. Downstream of the target, the beam enters the field of a strong, vertical sweeping magnet (B7), the gap of which is filled with tungsten-alloy inserts containing a passage for the neutral beam. This passage is shaped to absorb the remaining primary protons at a point where they are separated from the neutral beam, and to intercept the curved trajectories of all charged secondary particles from the target. The magnet is followed by a steel collimator, which is fitted with further precisely-bored inserts, ranging from a beam defining aperture of 3.6 mm at 4.8 m from the target to a final diameter of 6.0 mm at the exit, 6.0 m after the target, where the K_S beam enters the decay volume. The overall length of the K_S collimator is close to the optimum of $1c\tau_S$, where the ratio of useful K_S flux to neutron- and photon-induced background from the defining aperture is maximum. Moreover, according to a test made with the target moved out of the beam, the collimator ensures that, with the exception of muons, $\sim 85\%$ of the single-particle rates and $\sim 95\%$ of the two-particle coincidences recorded by the principal detectors are associated with protons striking the target (as opposed to originating from those dumped in the collimator).

6.4 Parameters and performance

The principal parameters and expected performance of the proposed dedicated, intense K_S beam are listed and compared to the present, simultaneous K_L and K_S beams in Table 4. The counting rates given in the Phase I version of the beam are quoted for 5×10^9 primary protons per pulse and are based on measurements made in the course of a brief test in 1999. We note that during this test the iridium-crystal photon-converter of the AKS anti-counter array present at the exit of the K_S collimator was removed, but the counters (representing ~ 15 mm thickness

of scintillator) remained in place and the sweeping magnet (B7) was operated at $\sim 2/3$ of its maximum strength.

With respect to the present test performed in 1999 we propose to make the following improvements to the dedicated, intense K_S beam:

1. Dismount the whole AKS anti-counter array at the exit of the K_S collimator and establish a continuous vacuum along the passage of the beam;
2. Introduce a 1.5 m long absorber plug made of bronze into the present K_L -beam aperture below the K_S beam in the final collimator (Figure 4);
3. Operate the K_S -beam sweeping magnet at maximum strength ($\sim 7.5 \text{ T} \cdot \text{m}$).

These improvements can readily be made for a data-taking period which may precede the completion of the $\Re(\epsilon'/\epsilon)$ measurement (Phase I in Table 4). Once the $\Re(\epsilon'/\epsilon)$ measurement has been completed, two further improvements designed to extend the sensitivity of the rare-decay programme are proposed (Phase II in Table 4):

4. Request and exploit a 50% longer SPS proton duty cycle, similar to the one used for high-energy ion physics, with a spill time of $\sim 5 \text{ s}$ at 400 GeV/c momentum every 19.2 s;
5. Exchange the proton steering magnet just upstream of the K_S target (B6 in Figure 4 by a stronger magnet, in order to reduce the production angle of the beam to $\sim 2.5 \text{ mrad}$ compared to the present 4.2 mrad.

These measures should allow the primary proton flux to be increased to 1×10^{10} per pulse and a single-event-sensitivity per year of $\sim 3 \times 10^{-10}$ to be reached, assuming a 10% detection efficiency. With these conditions the instantaneous rate in the principal detectors would be limited to ~ 1.5 times those currently observed from the simultaneous $K_L + K_S$ beams (Table 4). The expected momentum spectra of the K_S 's leaving the collimator and decaying in the fiducial region are shown in Figure 6 (a) for Phase I, and (b) for "Phase II", respectively. For Phase II, the lifetime distribution of the K_S decaying beyond the end of the collimator is plotted in Figure 7. We have verified that all of these improvements can be realised without incurring significant cost.

7 Detector and front-end electronics

The main components of the detector (see Figure 5) consist of a high resolution NA48 liquid krypton calorimeter (LKr) and magnetic spectrometer. To pre-trigger on charged decays, a plastic scintillator charged hodoscope (CHOD) is used. The hadron calorimeter is used to keep the pre-trigger rate low enough to strobe the Level II charged trigger and to reconstruct hadronic energy.

A set of seven anti-counter rings (AKL) surrounding the vacuum decay tank is used to veto charged and neutral particles escaping from the fiducial region. A muon filter at the end of the hall allows the identification of pion decays and provides a two-muon trigger.

We have measured counting rates during two short high-intensity K_S tests performed in 1999, and have compared these rates with the ones occurring during the $\Re(\epsilon'/\epsilon)$ runs. The results are shown in Table 4.

The rate increase in the AKL detector is larger than for other detectors. The reason is that the first ring of anti-counters is quite close to the K_S target station and therefore subtends a

large solid angle. We will remove the first ring from the anti-trigger to avoid larger random veto. For all other detectors the rates are within a factor 1.5 with respect to the standard $\mathfrak{R}e(\varepsilon'/\varepsilon)$ running situation, and therefore we do not anticipate rate problems in the detectors.

A test made during a special run conducted at the end of the 1998 proton data taking confirmed that the LKr calorimeter can be run at larger particle flux (at least four times larger) than the standard $\mathfrak{R}e(\varepsilon'/\varepsilon)$ operation.

The ultimate increase in kaon flux in the detector will be determined by the current drawn by the drift chambers. The use of a faster pre-amplifier would allow us to reduce significantly the current drawn for the same number of incoming protons. A more detailed discussion on this subject is given in Section 9.3.

8 Trigger

The main counting rate is generated by genuine $K_S \rightarrow \pi\pi$ and hyperon decays. A detailed description of the NA48 neutral and charged triggers exist [13]. We recall in this document only the essential information. A multi-stage trigger is used consisting of a pre-trigger, a Level II trigger, and a Level III trigger. The pre-trigger, based on information from the hodoscope and the calorimeters, is used to strobe the Level II charged trigger. This trigger is based on a processor farm which performs the reconstruction of the event in terms of the vertex and invariant masses of the charged tracks. The input rate to the Level II is 100 KHz, limited by the extraction of data from the drift chamber (DCH) read-out and by the amount of time available to perform the calculations. The neutral Level II trigger, digitises the LKr data from 128×2 projections and calculates the total energy, the centre of gravity and the proper time for the decayed kaon. In addition, there is provision to count the number of peaks in each projection. The maximum Level II rate which could be tolerated by NA48 turned out to be 7.5 KHz. This figure limits the physics range of the proposed search. We have identified certain bottlenecks and in principle with a minor upgrade of the read-out systems we feel that the sustainable rate could be increased from 7.5 to 15 KHz. Details of these possible upgrades are described in Section 9. We plan to reduce the raw data size by a factor of ~ 3 by applying a further Level III trigger in the central data recording (CDR) reconstruction farm.

1. $K_S \rightarrow 3\pi^0$

A selective $3\pi^0$ trigger is obtained by requiring more than 4 peaks in at least one projection. The measured trigger rate amounts to 1500 for 10^{10} protons on target. However, this cut on the number of peaks entails a $\sim 7\%$ inefficiency. To obtain full efficiency, one would want to apply the cuts based on the number of peaks in the Level III trigger where the full two dimensional capability of the LKr can be exploited. This possibility would also allow a sensitive search for the $K_S \rightarrow \pi^0\pi^0\gamma$ channel to be made. With no cut on the number of peaks, the neutral trigger rate would amount to ~ 15000 counts. This rate would almost saturate the current available band-width by itself, so this looser trigger can be employed only if the upgrade described in Section 9.1 is implemented.

2. $K_S \rightarrow \pi^0 e^+ e^-$

The final state for this decay is purely electro-magnetic and can be triggered by the calorimeter. To distinguish the final state from the $2\pi^0$ final state, one requires at least one hit from the drift chamber multiplicity trigger (which is based on drift chamber 1). The rate for this trigger is high: 5000 counts for 10^{10} protons on target. The rate may be

reduced by requiring at least 2 hits in the first drift chamber. The drawback of this option is that the efficiency for $K_S \rightarrow \gamma e^+ e^-$ may be reduced significantly.

3. $K_S \rightarrow \gamma\gamma$

In addition to a very short vertex decay region (as explained in section 3), a condition of no more than 3 peaks in both projections keeps the trigger rate at a reasonable level.

4. $K_S \rightarrow \pi^0\gamma\gamma$

This is the channel which has the greatest overlap with the copious $2\pi^0$ final state. Success therefore depends upon our ability to reject the unwanted $2\pi^0$ channel in the Level III trigger. However, this requires improving the frequency at which the LKr can be read out. Although no principle problem is foreseen, this will require the upgrade of the LKr read-out as outlined in Section 9.

5. The 4 track trigger

The 4 track trigger requires the presence of at least 2 reconstructed vertices within a short distance from each other. It has been used successfully during NA48 data-taking, and allows us to trigger on various decay modes, including $K_S \rightarrow \pi^+\pi^-e^+e^-$, $K_S \rightarrow e^+e^-e^+e^-$, and $K_S \rightarrow \mu^+\mu^-e^+e^-$.

The overall rate for 10^{10} protons on target is about 2000 counts.

6. The hyperon trigger

For the hyperon pre-trigger we required during the test run 1999 at least one coincidence between the two planes in the charged hodoscope in addition to a minimum total energy signal from the calorimeters and at least two hits from the first drift chamber.

In the second level charged trigger, we required a relaxed closest distance of approach (cda) cut to determine the vertex. The relaxed cda cut (at 8 cm) allows us to trigger on semi-leptonic Ξ^0 decays.

In order to reject the dominant $K_S \rightarrow \pi^+\pi^-$ decays, a cut on the invariant mass of the two charged tracks (assumed to be pions) is applied around the K_S mass. To exploit the presence of the baryon in the final state, the ratio of the momenta of the two tracks is required to be greater than 5 or smaller than 1/5.

The rate for this trigger is high: 50000 counts for 10^{10} protons on target. We plan further studies to reduce the trigger rate. We note, however, that the trigger is already very rich in hyperons (30%) and it may be difficult to do reduce the rate without deliberate down-scaling.

7. Control triggers

Normalisation is provided by samples of two-pion K_S decays. In addition, there are control triggers to determine the efficiency of the physics triggers.

9 Read-out systems

The NA48 read-out systems will be used. During the $\Re(\epsilon'/\epsilon)$ data taking, 250 Mb of data were read out for every SPS cycle (2.5 s duration). The typical size of one event was 14 kb, corresponding to an average trigger rate of 7.5 KHz. The read-out as it stands allows us to achieve the sensitivity specified in Section 2 for the $K_S \rightarrow \pi^0 e^+ e^-$ channel. However, to exploit

fully the physics reach of the proposed experiment, we have studied the NA48 read-out systems and we have identified a few bottlenecks that can be overcome.

9.1 LKr read-out

A description of the NA48 LKr read-out has been published [11]. The LKr calorimeter is read out by 40 MHz 10-bit FADC's. The dynamic range is further extended to 14 bits by means of a gain switching technique [12]. The detector is continuously digitised at 40 MHz and stored in a circular buffer which over-writes every 200 μ s. Upon receipt of a Level II trigger (time stamp command), the data are moved to another buffer where they wait to be read out. One read-out module (CPD) houses 64 channels. The read-out command activates the transfer of the data stored in the linear buffer of the CPD to the Data Concentrator (DC) via an optical link. The Data Concentrator performs the zero suppression according to a halo expansion algorithm. In the standard $\Re(\epsilon'/\epsilon)$ -mode read-out sequence, 10 samples are transferred from the CPD to the DC. The first two samples are completely unbiased by the presence of the signal and are therefore used to measure the pedestal on an event by event basis. This allows accidental activity preceding the event to be identified. The pulse related to the triggered event is found typically in samples 5, 6, 7, and 8. The first bottleneck in the read-out chain is due to the transfer time from the CPD to the DC. For the K_S experiment, we plan to reduce the number of samples read out from 10 to 8 or fewer. We are currently evaluating the loss in resolution implied by a further reduction of the number of read-out samples to a minimum of 4 samples. This can reduce the transfer time from 40 to 20 μ s. The second bottleneck is related to the DC pipeline which is clocked at 10 KHz. This limitation can be avoided by combining more than one event per read-out operation from the CPD to the DC. The proposed scheme requires modifications to the event building software and a hardware upgrade. The cost has been evaluated (see section 11).

9.2 The Hadronic Calorimeter read-out

During the K_S test it was noted that the hadronic calorimeter (HAC) read-out becomes a limiting factor if more than 9000 triggers per burst are read out. It is found that the hyperon triggers are very rich in hadronic energy and therefore create a large amount of data. We plan to double the read-out modules (CPD) from 4 to 8, and to increase the number of RIO computers to speed up the zero suppression algorithm and reduce the data load. The cost of implementing this option is evaluated in section 11.

9.3 The DCH read-out

The NA48 drift chamber read-out suffers from a limitation in the number of hits that can be stored. Although in principle up to 16 hits can be stored for each plane, in practice this limit is set to 7. This limit is chosen to avoid uncontrolled truncation in the downstream end of the DCH readout. When more than 7 hits in a plane are detected within 100 ns, an overflow (OFL) signal is issued. In the presence of an OFL, the read-out may be truncated. The $\Re(\epsilon'/\epsilon)$ analysis has demonstrated that to insure good trigger and reconstruction efficiency, no OFL must be present in a window of ± 300 ns around the time of the event. This creates an effective dead time in the $\Re(\epsilon'/\epsilon)$ experiment as high as 25%. We are studying the impact of this OFL problem for the K_S programme. Although we expect a single rate in the detectors comparable to or larger than that in the $\Re(\epsilon'/\epsilon)$ experiment, the situation may be better as far as the OFL is concerned. This is because the main source of OFL is due to EM showering particles in the

material preceding the DCH. In the $\Re(\varepsilon'/\varepsilon)$ experiment, 40% of the K_L 's decays into $\pi^\pm e^\mp \nu$ with an electron shower, and 20% decay into $3\pi^0$. In addition, many of the decays originate well downstream of the interesting decay region. For K_S , the situation is better since there are few decays occurring downstream of the fiducial decay region. However, we are evaluating the possibility of reducing the event loss due to OFL by increasing the buffer memory of the RING cards to allow a larger number of TDC hits to be stored.

10 DAQ system

We propose to use the NA48 online and CDR system. The system is based on 24 Pentium PCs and allows event-building up to 400 Mb per cycle. The CDR/L3 system in the IT building would be needed to handle the large amount of data foreseen. We will run Level III active triggers to provide a substantial reduction of the raw data (a factor of three is planned).

11 Estimated cost and request for beam time

In November 1999 the NA48 beam pipe imploded damaging the four drift chambers. A plan for the repair is being worked out and here we assume that the four chambers will become operational by the year 2001. Details of the cost and time schedule for the repair can be found in [14]. Parts of this proposal concerning K_S decays with charged particles cannot be executed before the chambers will be repaired. On the other hand, the measurements described in sections 3 and 4 profit from the absence of the drift chambers, since the limitation on the kaon flux due to the counting rate in the drift chambers does not apply. We could start the data taking for the neutral decays in the year 2000 before the completion of the $\Re(\varepsilon'/\varepsilon)$ experiment. Once the $\Re(\varepsilon'/\varepsilon)$ experiment will be completed, we would like to run for one more year to reach the proposed sensitivities.

As stated above, the sensitivity of the current proposal can be improved by a factor of two, if an upgrade of the read out system for the drift chambers and for the LKr calorimeter is performed. The costs involved in this operation are outlined in Table 5.

The sensitivity of such a programme benefits by $\sim 50\%$ by adopting a long SPS proton duty cycle, similar to the one used for ion physics, giving a spill time of 5 s. at 400 GeV/c momentum every 19.2 s. It is our understanding that NA58 (COMPASS) have a similar interest and we ask the SPSC to encourage the introduction of this cycle for Phase II of this proposal.

The Orsay group will participate in the $\Re(\varepsilon'/\varepsilon)$ tests that will take place in 2000 and will continue to assume responsibility for its detectors during the whole 2000 run, including the high intensity KS part.

12 Competition

The competition to this experiment comes from the KLOE detector. However, even at the full DAPHNE design luminosity of $5 \times 10^{32} \text{ cm}^{-2}\text{s}^{-1}$, the sensitivity per annum for $K_S \rightarrow \pi^0 e^+ e^-$ is less than this proposal. At present, the DAPHNE luminosity is less than 1% of design. Unlike KLOE, we cannot tag our K_S , thus making the two experiments complementary to some extent.

References

- [1] G. D'Ambrosio, G. Ecker, G. Isidori, and J. Portoles Published in JHEP 9808:004,1998 e-Print Archive: hep-ph/9808289.
- [2] J. Kambor and B.R. Holstein, Phys. Rev. D49, 2346 (1994).
- [3] G.B. Thomson, Y. Zou, Phys. Rev. D51 1412 (1995).
- [4] A. Angelopoulos *et al.* (CPLEAR Collaboration), Phys. Lett. B425 391 (1998).
- [5] M.N. Achasov *et al.* (SND Collaboration), Phys. Lett. B459 674 (1999).
- [6] A. Duncan, E. Eichten and T. Thacker, Nucl. Phys. Proc. Suppl., 53, 299 (1997).
- [7] Review of particle physics. Eur. Phys. J. C3 1 (1998).
- [8] P. Zenczykowski, Phys. Rev. D40, 2290 (1989).
- [9] C. Biino, N. Doble, L. Gatignon, P. Grafstrom and H. Wahl," The Simoultaneous Long- and Short-lived Neutral Kaon Beams", CERN-SL98-033 (EA) and Note 98-16, updated September 1999
- [10] N. Doble, L. Gatignon, P. Grafstrom, Nucl. Instr. Meth. B119, 181 (1996).
- [11] O. Vossnack, Calorimetry in High Energy Physics, Tucson, Arizona, USA, page 420-428, World Scientific (1997).
- [12] B. Hallgren et al, Nucl. Instr. and Meth, A, 419,680 (1998)
- [13] "A 40 MHz Pipelined Trigger for $K_0 \rightarrow 2\pi^0$ Decays for the CERN NA48 Experiment", G. Fischer et al., Nucl. Instr. Meth. A419, 695 (1998).
"The charged trigger system of NA48 at CERN", S. Anvar et al., Nucl. Instr. Meth. A419, 686 (1998).
- [14] " Memorandum: Plan to repair the NA48 drift chambers", in preparation.

K _S decay mode	K _S			Expected background from K _L			Comments
	Expt. B.R.	Theor. B.R.	N ^o of events per year ^a (assumed acceptance)	Expt. B.R.	Theor. B.R.	N ^o of events per K _S lifetime per year	
$\pi^0 e^+ e^-$	$< 1.1 \times 10^{-6}$	$\sim 5 \times 10^{-9}$	7 (5%)	$< 5.64 \times 10^{-10}$	$\sim 1.5 \times 10^{-11}$	0	Indirect \mathcal{CP} contrib. to $K_L \rightarrow \pi^0 e^+ e^-$
$\pi^0 \mu^+ \mu^-$		$\sim 1 \times 10^{-9}$	~ 3 (10%)	$< 3.4 \times 10^{-10}$	$\sim 3 \times 10^{-12}$	0	Indirect \mathcal{CP} contrib. to $K_L \rightarrow \pi^0 \mu^+ \mu^-$
$\gamma\gamma$	$(2.4 \pm 0.9) \times 10^{-6}$	2.1×10^{-6}	24000 (30%)	$(5.92 \pm 0.15) \times 10^{-4}$ (110000)		25000	Unambiguous prediction by χ PT
$\gamma e^+ e^-$		3.4×10^{-8}	204 (20%)	$(9.1 \pm 0.5) \times 10^{-6}$		255	
$\gamma \mu^+ \mu^-$				$(3.25 \pm 0.28) \times 10^{-7}$		9	
$\pi^0 \gamma\gamma$		3.8×10^{-8} ($m_{\gamma\gamma} > 220$ MeV)	114 (10%)	$(1.70 \pm 0.28) \times 10^{-6}$		23	
$\pi^0 \pi^0 \pi^0$	$< 1.9 \times 10^{-5}$	2.52×10^{-9}	4 (5%)	0.2112 ± 0.0027		1.5×10^6	CPT test and violation
$\pi^0 \pi^0 \gamma\gamma$		5×10^{-9} ($ m_{\gamma\gamma} - m_\pi > 20$ MeV)	7 (5%)		3×10^{-8}	$\lesssim 1$	Probes the momentum dependence of $K\pi^0\pi^0$ vertex
$\pi^0 \pi^0 \gamma$		1.7×10^{-11}	0 (5%)	$< 5.6 \times 10^{-6}$	7×10^{-11} or 1×10^{-8}	0	
$\pi^+ \pi^- \gamma$ (int. Brem.)	$(1.78 \pm 0.05) \times 10^{-3}$	1.75×10^{-3} ($E_\gamma^* > 50$ MeV)	5.3×10^6 (10%)	$(4.61 \pm 0.14) \times 10^{-5}$		640	Look for departures from brems. spect.
$\pi^+ \pi^- \gamma$ (dir. emm.)	$< 9 \times 10^{-5}$	$\sim 10^{-6}$ ($E_\gamma^* > 50$ MeV)	3000 (10%)				
$\pi^+ \pi^- \pi^0$	$(3_{-1.0}^{+1.2}) \times 10^{-7}$	$(2.4 \pm 0.7) \times 10^{-7}$	1350 (15%)	0.1256 ± 0.0020		2.6×10^6	
$\pi^+ \pi^- e^+ e^-$		3.6×10^{-5}	54000 (5%)	$(2.90 \pm 0.15) \times 10^{-7}$	$\sim 3 \times 10^{-7}$	2	
$\mu^+ \mu^-$	$< 3.2 \times 10^{-7}$	$O(10^{-11})$		$(7.2 \pm 0.5) \times 10^{-9}$		0	
$e^+ e^-$	$< 1.4 \times 10^{-7}$			$(9_{-4}^{+6}) \times 10^{-12}$		0	

^aAssuming no upgrade to detectors or readout.

Table 1: Rare K_S decays accessible to this experiment and contamination from K_L decays in the beam.

Decay mode	α_f	$10^3 \times \text{Re}(\alpha_f)$	$10^3 \times \text{Im}(\alpha_f)$
$K_L \rightarrow \pi^+ \pi^-$	$\alpha_{+-} = \mathcal{B}_{+-}^{(S)} \eta_{+-}$	1.137 ± 0.015	1.079 ± 0.016
$K_L \rightarrow \pi^0 \pi^0$	$\alpha_{00} = \mathcal{B}_{00}^{(S)} \eta_{00}$	0.519 ± 0.011	0.491 ± 0.011
$K_L \rightarrow \pi^+ \pi^- \gamma$	$\alpha_{+-\gamma} = \mathcal{B}_{+-\gamma}^{(S)} \eta_{+-\gamma}$	< 0.001	< 0.001
$K_L \rightarrow \pi l \nu$	$\alpha_{l3} = \frac{\tau_S}{\tau_L} [\mathcal{B}_{\pi\mu\nu}^{(L)} + \mathcal{B}_{\pi e\nu}^{(L)}] \times$ $[\delta_l(1 + \text{Re}(x)) - 2i\text{Im}(x)]$	0.004 ± 0.001	0.007 ± 0.059
$K_S \rightarrow \pi^+ \pi^- \pi^0$	$\alpha_{+-0} = \frac{\tau_S}{\tau_L} \mathcal{B}_{+-0}^{(L)} \eta_{+-0}$	0.000 ± 0.002	0.000 ± 0.002
$K_S \rightarrow \pi^0 \pi^0 \pi^0$	$\alpha_{000} = \frac{\tau_S}{\tau_L} \mathcal{B}_{000}^{(L)} \eta_{000}$	0.062 ± 0.044	0.026 ± 0.055
$(1 + i \tan \phi_{\text{SW}}) \text{Re}(\epsilon)$		1.635 ± 0.060	1.551 ± 0.057
Difference $\sum_f \alpha_f - (1 + i \tan \phi_{\text{SW}}) \text{Re}(\epsilon)$		0.087 ± 0.077	0.052 ± 0.101

Table 2: All the α_f that contribute to the Bell-Steinberger relation and their current best values (from [7]). $\mathcal{B}_f^{(S),(L)}$ are the branching ratios of K_S, K_L into the final state f . δ_l is the charge asymmetry in semileptonic decays and x is the $\Delta S = \Delta Q$ violation parameter.

decay mode	Comment	Branching ratio ($\times 10^{-3}$)
$\Xi^0 \rightarrow \Sigma^+ e^- \bar{\nu}_e$	625 evts	$0.254 \pm 0.011 \pm 0.016$
$\Xi^0 \rightarrow \Sigma^+ \mu^- \bar{\nu}_\mu$	DPF, KTEV (preliminary)	$(2.6_{-1.7}^{+2.7} \pm 0.6) \times 10^{-3}$
$\Lambda \rightarrow p e^- \bar{\nu}_e$	7000 evts	0.832 ± 0.014
$\Lambda \rightarrow p \mu^- \bar{\nu}_\mu$	18 evts	0.157 ± 0.035
$\Xi^0 \rightarrow \Lambda \gamma$	BR and asymmetry	1.06 ± 0.16
$\Xi^0 \rightarrow \Sigma^0 \gamma$	BR and asymmetry	3.5 ± 0.4
$\Sigma^0 \rightarrow \Lambda \gamma \gamma$	not seen yet, search	
$\Xi^0 \rightarrow p \pi^-$	$\Delta S = 2$ transition, improve best limit	$< 4 \times 10^{-5}$
	M_{Ξ^0} improve mass measurement M_{Ξ^0} not measured yet Ξ^0 -Lifetime worst known for all hyperons Polarisation of Ξ^0 and Λ and anti particles CPT tests on masses and lifetimes	Error: 3%

Table 3: Some rare hyperon decays accessible to this experiment.

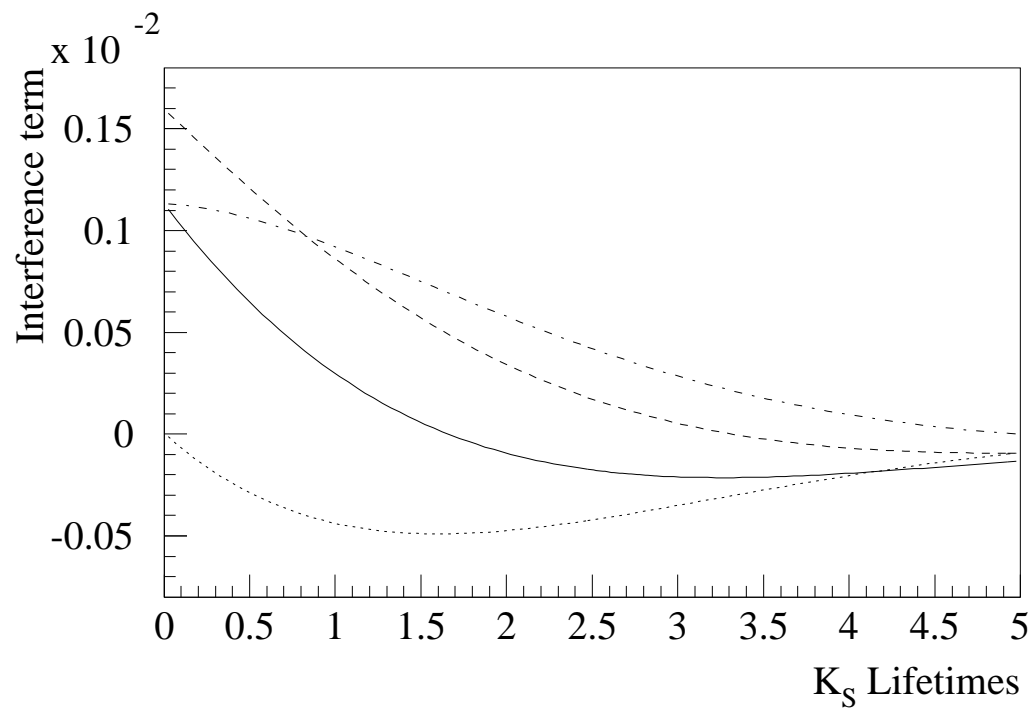


Figure 1: The interference term for the first 5 K_S lifetimes. The phases are $\phi_{000} = 45^\circ \approx \phi_{000}$ (solid), $\phi_{000} = 0^\circ$ (dashed), $\phi_{000} = 90^\circ$ (dotted), and $\phi_{000} = -45^\circ$ (dash-dotted). $I_{3\pi^0}$ has been normalized to 1 at $t = 0$.

Beam	$K_L + K_S$ (ϵ'/ϵ)		Intense K_S beam	
Year	1999-2000		Phase I	Phase II
Installation Changes	—		<ul style="list-style-type: none"> • remove AKS • plug K_L final coll. 	<ul style="list-style-type: none"> • replace magnet upstream of K_S-target
SPS momentum (GeV/c)	450		450	400
Duty Cycle (s/s)	2.5/14.4		2.5/14.4	5.0/19.2
Protons per pulse on target	1.5×10^{12}	3×10^7	5×10^9	1×10^{10}
Production angle α (mrad)	+2.4	-4.2	-4.2	-2.5
Length (m) target—final coll.	126	6.0	6.0	
Distance (m) final coll.—LKr cal.	115		115	
Beam acceptance angle $\pm\theta$ (mrad)	± 0.15	± 0.375	± 0.375	
Solid Angle Ω (sterad $\times 10^{-8}$)	2.25π	14.0π	14.0π	
Mean momentum \bar{p}_K (GeV/c)	~ 110		~ 110	~ 115
Useful mom. range Δp_K (Gev/c)	70-170		40-240	
Total beam flux K's/pulse	$\sim 2 \times 10^7 + \sim 3 \times 10^2$		$\sim 5 \times 10^4$	$\sim 1.5 \times 10^5$
K-decays in Δp_K /pulse	$1.0 \times 10^5 + 1.8 \times 10^2$		4.0×10^4	1.1×10^5
K-decays in Δp_K /year ($\frac{1}{2} \times 120$ days)	$3.6 \times 10^{10} + 6.5 \times 10^7$		1.4×10^{10}	3.0×10^{10}
CHOD	Qor	2.3	3	~ 9
Rates $\times 10^6$ /pulse	Qh.Qv	1.4	1.5	~ 4.5
	Qx	0.75	0.75	~ 2.2
Inst'ous	Qor	~ 1.5	~ 2	~ 3
Rates $\times 10^6$ /s eff. spill	Qh.Qv	~ 0.9	~ 1.0	~ 1.5
	Qx	~ 0.5	~ 0.5	~ 0.75

Table 4: Parameters and performance of intense K_S beam compared to present $K_L + K_S$ beams.

system	Estimated cost (KSfr)
LKr read out	
Upgrade of the DT/SLINK interfaces	25
Assembly of 10 CPD spares (4 for the HAC)	60
Reprogramming of CPD FPGA	20
DCH front end and read out	
Modification of preamplifier	40
New cables to TDC	30
Design and construction of 32 new TDC-RING cards	under evaluation

Table 5: Cost estimate for the proposed upgrade.

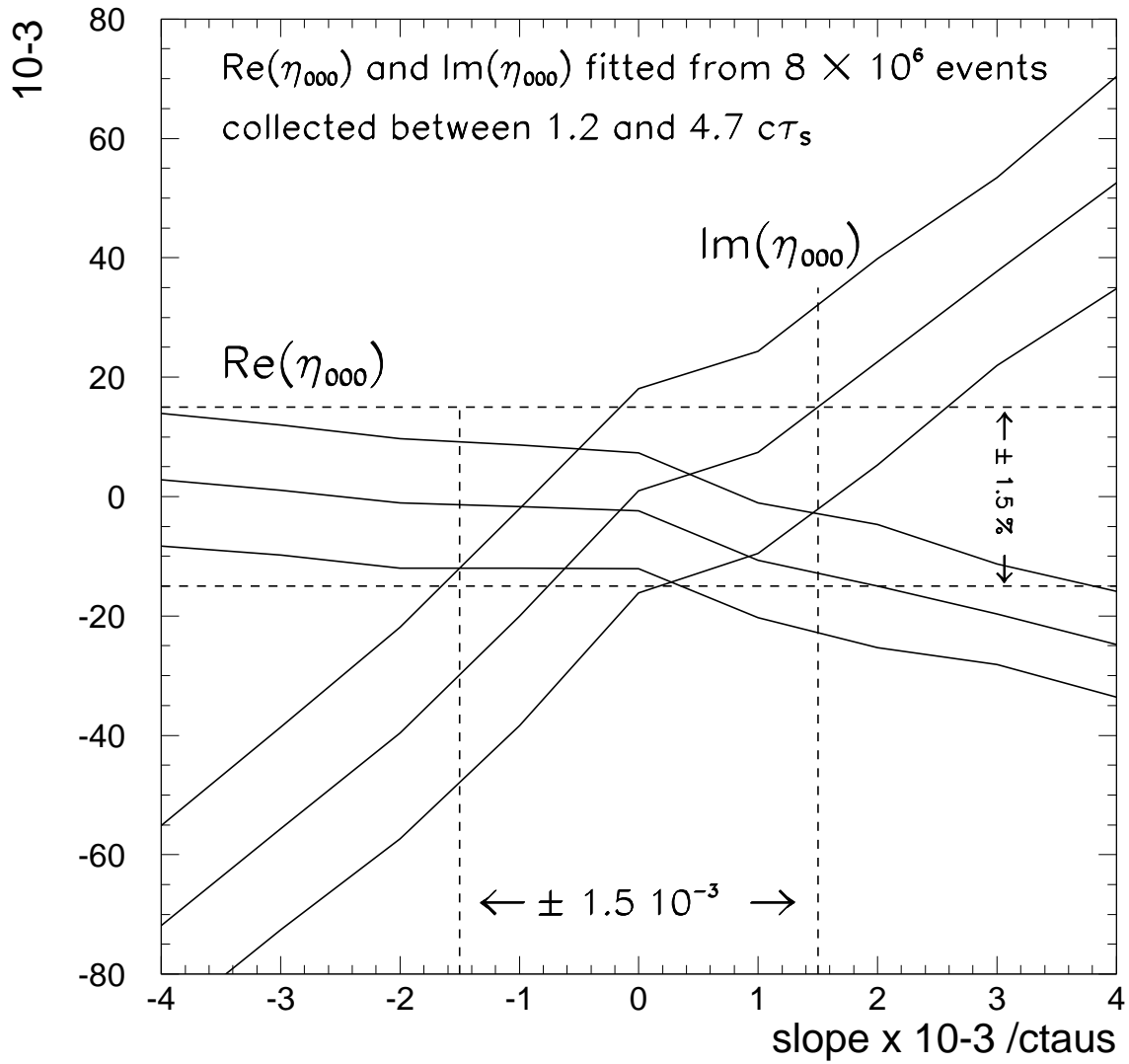


Figure 2: Statistical error on η_{000} and systematic error due to limited knowledge of the acceptance ($\phi_{000} = 45^\circ$)

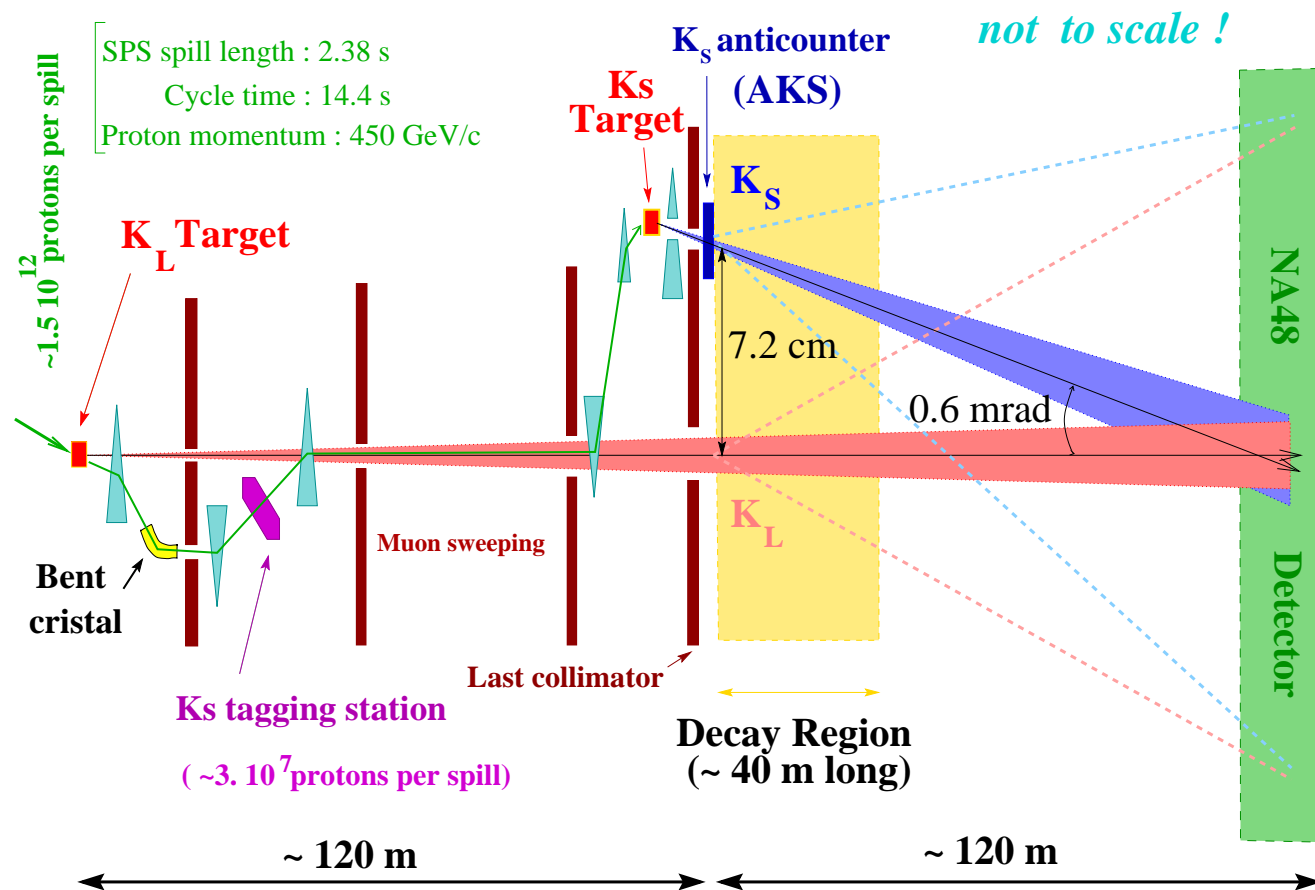


Figure 3: A schematic layout of the K_L and K_S beams (vertical section)

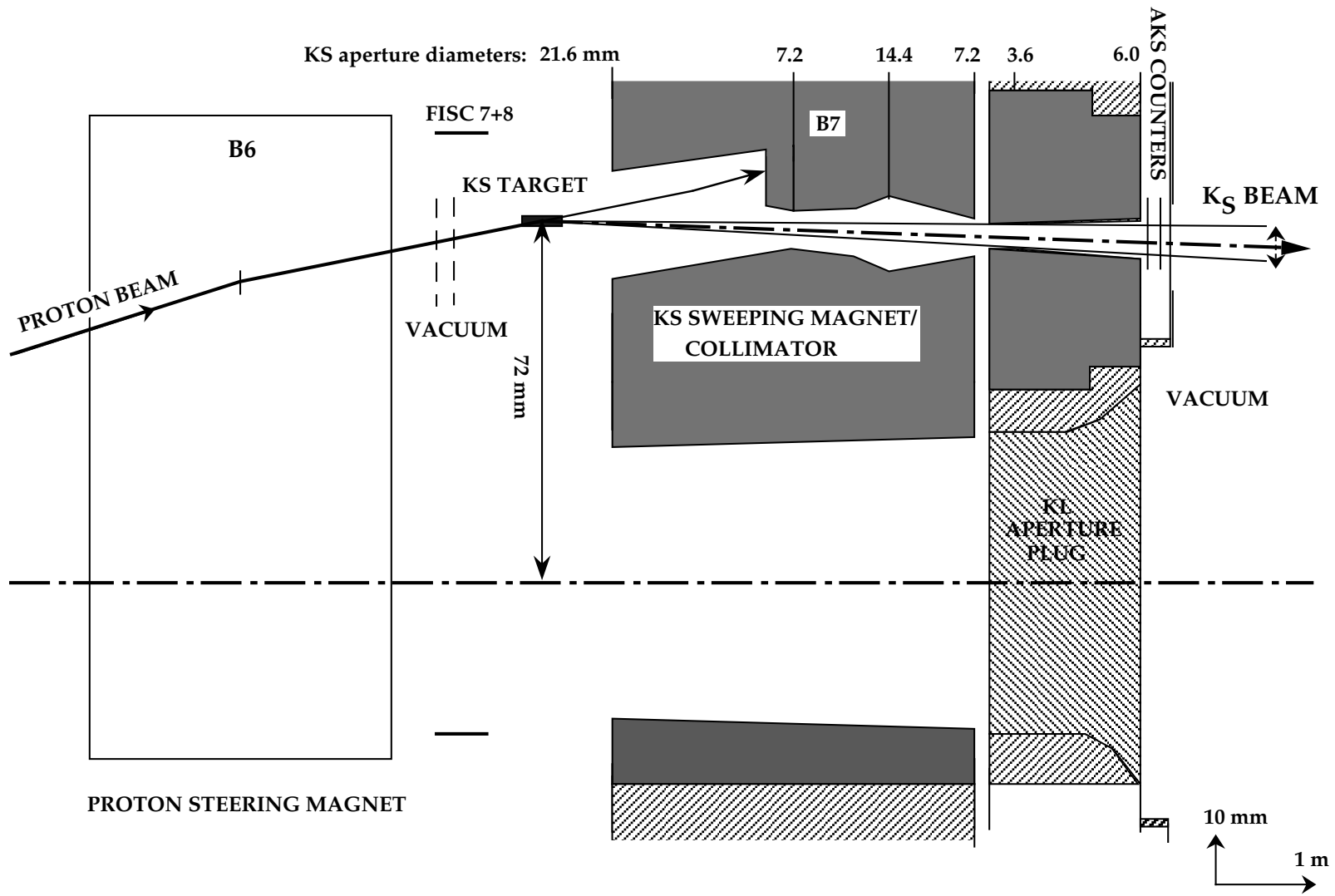


Figure 4: Detailed layout of the K_S target station and beam (vertical section)

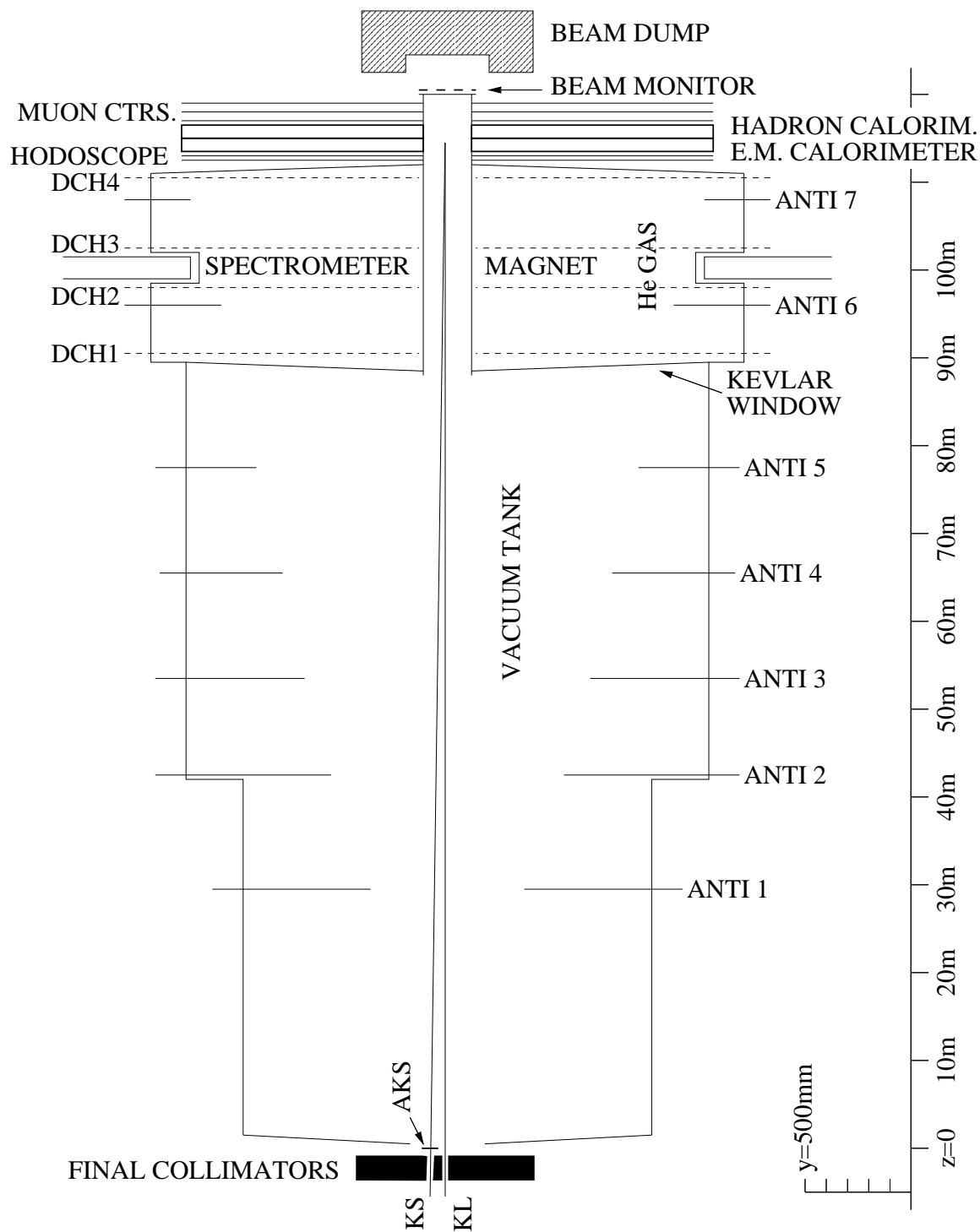


Figure 5: Layout of the NA48 detectors

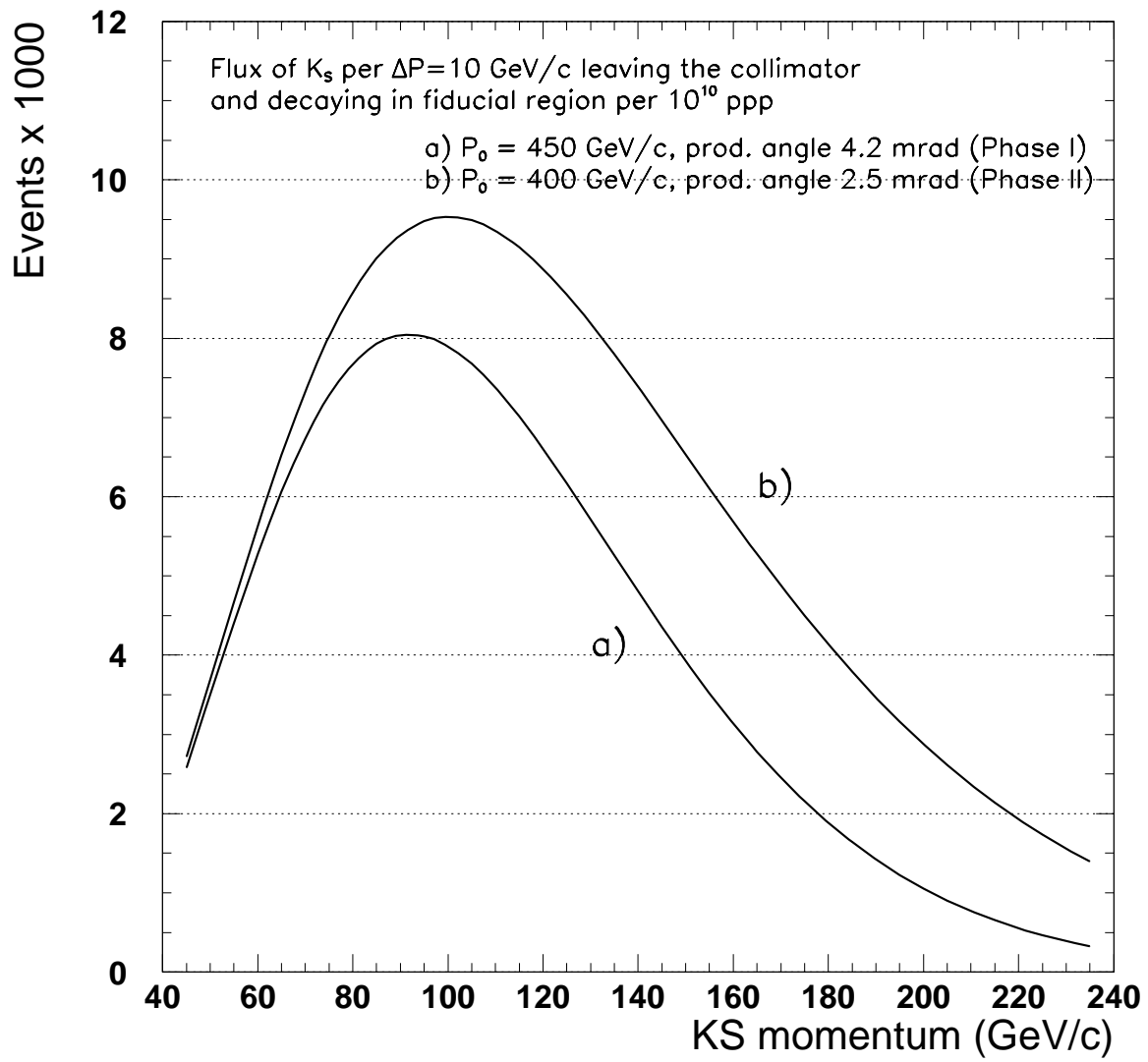


Figure 6: Flux of K_S into the decay region versus momentum

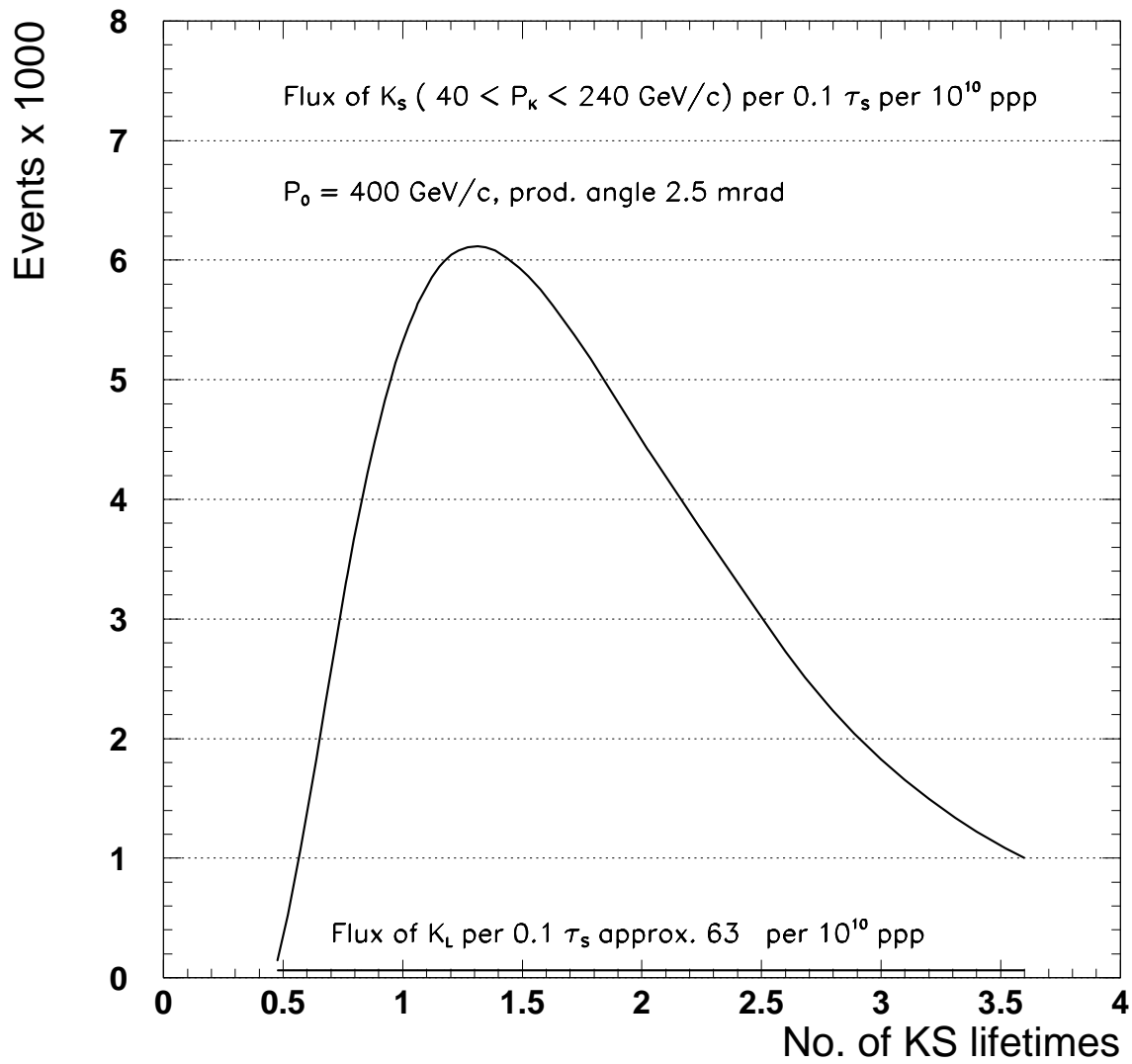


Figure 7: Flux of K_S into the decay region versus lifetime